Toxicology in Vitro 26 (2012) 7–15

Contents lists available at SciVerse ScienceDirect

Toxicology in Vitro

journal homepage: www.elsevier.com/locate/toxinvit

The new murine hepatic 3A cell line responds to stress stimuli by activating an efficient Unfolded Protein Response (UPR)

Barbara Guantario [a], Alice Conigliaro [b], Laura Amicone [b], Yula Sambuy [a], Diana Bellovino [a,*]

[a] National Research Institute on Food and Nutrition (INRAN), Rome, Italy
[b] Department of Cellular Biotechnologies and Haematology, University "La Sapienza", Rome, Italy

ARTICLE INFO

Article history:
Received 10 June 2011
Accepted 26 September 2011
Available online 4 October 2011

Keywords:
Cellular model
Hepatocytes
ER stress
RBP4

ABSTRACT

In the present study we have investigated the properties of a novel cell line (3A cells) obtained from the liver of 14.5 days *post coitum* (dpc) wild-type mouse embryo. 3A cells morphology was characterized by fluorescent localization of F-actin and β-catenin. The expression of specific genes and proteins essential to liver function in these cells was comparable or even more efficient then in the differentiated hepatocytic cell line MMH-D6. 3A cells also showed the capability to excrete molecules in extracellular spaces resembling functional bile canaliculi, glycogen storage activity and the ability to control retinol-binding protein 4 secretion in response to retinol deprivation. Their response to the exogenous stress stimulus induced by tunicamycin was analysed by PCR Pathway Array containing 84 genes involved in the Unfolded Protein Response (UPR). 3A cells were shown to activate the UPR following a typical stressful event, indicating that this cellular model could be further exploited to investigate hepatic proteins secretion and specific reaction to different injuries.

1. Introduction

The effort to establish a differentiated hepatic cell line able to express *in vitro* the most important liver functions (such as the synthesis of specific serum proteins, the metabolism of carbohydrates and lipids, and the modification and excretion of endogenous and exogenous molecules) has long been pursued in several laboratories and different model systems have been described to date (Ferrini et al., 1997; Gebhardt et al., 2003; Hewitt et al., 2007). Such *in vitro* systems are essential to test a wide panel of molecules, both of natural or synthetic origin, with beneficial (i.e. nutrients, bioactive molecules, drugs) or detrimental (i.e. environmental pollutants, metals, toxins, etc.) effects on the organism, and to study the molecular mechanisms that govern their absorption, metabolism, secretion and catabolism in the liver. Primary hepatocytes are still the closest *in vitro* model for the liver. However, they have scarce and often unpredictable availability, limited growth activity and lifespan, and undergo early phenotypic alterations (Guguen-Guillouzo and Guillouzo, 2010). Conversely, hepatoma cell lines such as HepG2, despite representing a widely used model characterized by indefinite proliferative capacity, lack several important regulatory mechanisms and crucial liver functions such as the cytochrome P450 activities (Guguen-Guillouzo and Guillouzo, 2010) or micronutrients transport (Bellovino et al., 1999; Pisu et al., 2005).

In this study we have characterized the 3A hepatic cell line, isolated from 14.5 dpc embryo of a wild type mouse strain that underwent spontaneous immortalization.

3A cells were tested for the maintenance of several liver key features essential for a functional hepatocyte model, including the regulation of retinol binding protein 4 (RBP4) secretion in response to vitamin A deficiency. In addition to structural and functional characteristics, we have tested their capability to overcome stressful conditions by activating the Unfolded Protein Response (UPR). The synthesis and secretion of large amounts of proteins such as hormones, antibodies or growth factors as well as various stresses, such as hypoxia, starvation, heat and drug treatment can interfere with proper protein folding in the endoplasmic reticulum (ER) (Kaufman et al., 2002) and consequently with protein secretion. These events lead to ER stress and accumulation of misfolded proteins that, in turn, can result in cell failure and death by apoptosis. Cells are able to activate specific pathways in order to prevent and relieve ER stress, in particular the UPR pathway, through which protein synthesis is inhibited and misfolded proteins are (i) detected, (ii) sequestered and/or re-folded, (iii) eventually degraded (Schroder and Kaufman, 2005; Ron and Walter, 2007). The correct functioning of this pathway ensures a proper response to exogenous stress, and is therefore essential for cells to exert efficiently their functions. A new, readily available cell model, easy to obtain and to maintain in culture, would therefore

* Corresponding author. Address: INRAN, Via Ardeatina 546, 00178 Rome, Italy. Tel.: +39 06 51494457; fax: +39 06 51494550.
E-mail address: bellovino@inran.it (D. Bellovino).

0887-2333/$ - see front matter © 2011 Elsevier Ltd. All rights reserved.
doi:10.1016/j.tiv.2011.09.020

be extremely useful for studies aimed at the characterization of the hepatic response to stressful events.

2. Materials and methods

2.1. Cell culture maintenance and drug treatment

The murine hepatocytes 3A cell line was derived from liver cultures of 14.5 dpc embryos of wild type mice by limiting dilution cloning. Met murine hepatocytes (MMH)-D6 is an immortalized cell line derived from livers of transgenic mice expressing a truncated human MET proto-oncogene. Details of the construction and of the tissue-specific and temporal expression of the transgene were previously published (Amicone et al., 1995). All cell lines were grown in RPMI 1640 supplemented with 10% foetal bovine serum (FBS EU category, Euroclone, Italy), 50 ng/ml EGF, 30 ng/ml IGF II (Millipore, Italy), 10 μg/ml insulin, 4 mM L-glutamine and 100 U/L penicillin and 100 μg/L streptomycin. Cells were usually plated on collagen I-coated Petri dishes (BD Falcon Plastics) at 37 °C in 5% CO_2.

To induce vitamin A deficiency, 3A cells were grown in RPMI 1640 supplemented with 10% delipidized FBS (Lonza, Basel, Switzerland). As control, 3A cells were grown in the same medium supplemented with 3 μM retinol, prepared as 1000× stock solution in ethanol. Where indicated, 3A cells were treated with 5 μg/ml tunicamycin (TM) for 4 h at 37 °C in 5% CO_2. Unless otherwise stated all reagents were from Sigma Aldrich, Italy.

2.2. RNA extraction, reverse transcription and PCR

Total RNA was extracted from cultured cells using an RNA extraction kit (NucleoSpins RNA II, Machery-Nagel GmbH, Germany) according to the manufacturer's instructions. Single-stranded cDNA was obtained by reverse transcription of 1 μg of total RNA using MMLV-reverse-transcriptase (Promega, Italy). cDNA was amplified by PCR using Taq DNA polymerase (Invitrogen, Italy). The samples were analysed by 1% agarose gel electrophoresis. The oligos used in the experiment were designed with *Primer3* software and the corresponding sequences are reported in Table 1.

PstI digestion was used to discriminate between the two different XBP1 mRNA splicing forms. 3A cells were treated with 5 μg/ml TM for 4 h at 37 °C, then total RNA was extracted from treated or control cells and used for RT-PCR amplification of XBP1 using specific primers. Amplified PCR fragments were digested with the restriction enzyme PstI (Promega, Italy) for 1 h at 37 °C. The samples were analysed by 1% agarose gel electrophoresis.

2.3. RT^2 Profiler PCR Array System

The Mouse Unfolded Protein Response RT^2 Profiler™ PCR Array (SABioscience-Qiagen, Italy) profiles the expression of 84 key genes responding to unfolded protein accumulation in the ER. Total cellular RNA was extracted from cultured cells (RNeasy® Mini Kit, Qiagen, Italy) according to the manufacturer's instructions. Single-stranded cDNA was obtained by reverse transcription of 1 μg of total RNA using SABiosciences RT^2 First Strand Kit. Real Time-qPCRs were performed using Applied Biosystems 7500 Fast with SYBR Green fluorophore; the reactions were carried out using iQt SYBRs Green Supermix (BioRad, Italy); cDNA was used as template and cycling parameters were 95 °C for 10 min, followed by 40 cycles of 95 °C for 15 s, 60 °C for 1 min. Fluorescence intensities were analyzed using the manufacturer's software, and relative quantification was calculated using the $2^{-\Delta\Delta Ct}$ method. HPRT1 was used as reference gene. Significant differences between treatments were evaluated using Student's *t*-test, with $p \leqslant 0.05$ considered significant.

2.4. Western blotting and immunoprecipitation

Cells were harvested in cold radioimmunoprotein assay (RIPA) buffer (20 mM Tris–HCl pH 7.5, 150 mM NaCl, 0.1% SDS, 1% Na deoxycholate, 1% Triton X-100, phosphatases and protease inhibitor cocktails (Roche, Italy)). Culture media, where indicated, were subjected to immunoprecipitation with anti-RBP4 antibody, followed by 1 h incubation with 30 μl of ProteinA-Sepharose (Roche). Sample aliquots were dissolved in sample buffer (50 mM Tris–HCl, pH 6.8, 2% SDS, 10% glycerol, 100 mg/ml bromophenol blue, 10 mM β-mercaptoethanol), heated for 5 min, fractionated by 4–20% SDS polyacrylamide gel electrophoresis (SDS–PAGE), then transferred to nitrocellulose filter. Membranes were incubated with the specific antibodies: rabbit polyclonal anti-albumin (Bethyl, Montgomery, TX, USA), rabbit polyclonal anti-RBP4 (Alexis-ENZO Life Science, Belgium), mouse monoclonal anti-tubulin (Sigma Aldrich, Italy), rabbit polyclonal anti-IRE1α, PERK and CHOP (Cell Signaling, Beverly, MA, USA). Proteins were then detected with horseradish peroxidase-conjugated secondary antibodies (Thermo Scientific, Rockford, IL, USA) and enhanced chemiluminescence (ECL) reagent (Perkin Elmer, Italy), followed by exposure to X-ray film (BioMax Light Film Kodak, Perkin Elmer, Italy). Densitometric analysis was performed by ImageQuantTL (GE Healthcare, Italy) software.

2.5. Immunofluorescence staining

3A cells were seeded on collagen-coated coverglasses. Cells were grown for 48 h after confluence and immunofluorescence performed as previously described (Conigliaro et al., 2008). Briefly, cells were fixed with 4% paraformaldehyde, permeabilized with 0.1% Triton X-100 and incubated with FITC-conjugated phalloidin or rabbit polyclonal antibodies against ß-catenin and albumin (Bethyl, Montgomery, TX, USA). Nuclei staining was performed with 1 μg/ml 4′,6-diamidino-2-phenylindole (DAPI). Coverglasses

Table 1
Primers used for RT-PCR analysis of the indicated genes.

Gene	Accession No.	Forward	Reverse
HNF1α	NM_009327.3	5′-AGACCATGTTGATCACAGAC-3′	5′-GGGTGGAGATAAAAGTCTCG-3′
HNF4α	NM_008261.2	5′-ACACGTCCCCATCTGAAG-3′	5′-CTTCCTTCTTCATGCCAG-3′
HNF3β	NM_010446.2	5′-ACATGTTCGAGAACGGCTGC-3′	5′-TGAAGGCTGAATGGTGCTCG-3′
HNF6	NM_008262.3	5′-GGGCTGGCCTCTATGAATAAC-3′	5′-GTTTGAGCTCGGTGGTGATAC-3′
GOT1	NM_010324.2	5′-AGCCTCAACCACCAGTACCT-3′	5′-ATCTGCTTCCACTGCCTCGG-3′
Ephx1	NM_010145.2	5′-TGGCTTCAACTCCAGCTACC-3′	5′-TTCTGACTTGGTCCAGGTGG-3′
E-Cad	NM_009864.2	5′-CAAGCTGGAGACCAGTTTCC-3′	5′-CAGAGGTGAGCACACTGATG-3′
RBP4	NM_001159487.1	5′-ACTGGGGTGTAGCCTCCTTT-3′	5′-GGAGTACTGCAGAGCGAAGG-3′
TTR	NM_013697.5	5′-CTGGACTGGTATTTGTGTCT-3′	5′-TTGGCTGTGAAAACCACATC-3′
XBP1	NM_013842.2	5′-AAACAGAGTAGCAGCTCAGACTGC-3′	5′-TCCTTCTGGGTAGACCTCTGGGAG-3′
β-actin	NM_007393.3	5′-ATGGATGACGATATCGCTGCG-3′	5′-ATCTTCATGAGGTAGTCTGTCAGG-3′

were mounted with ProLong Gold anti-Fade Reagent (Molecular Probes, Invitrogen, Italy) and visualized by confocal laser scanning microscopy (LSM-700, Zeiss, Jena, Germany).

2.6. Fluorescein-diacetate (FDA) staining

3A cells were grown for 48 h after confluence and incubated at 37 °C for 20 min with 5 μg/ml FDA in methanol. Cells were washed with PBS at room temperature and immediately visualized by fluorescence microscopy (Axioscope 2, Zeiss). Cell membranes were stained with Wheat Germ Agglutinin (WGA) Alexa-Fluor 555 conjugate (Molecular Probes, Invitrogen, Italy).

2.7. Periodic Acid Schiff (PAS) staining

Cell medium was replaced with fresh complete medium 2 h before analysis. Intracellular glycogen staining was performed using a PAS staining kit; before staining, control cells were incubated for 30 min at 37 °C with 10 mg/ml diastase (Roche). Fluorescent images of PAS-stained cells were captured using an EVOS microscope (AMG, Bothell, WA, USA).

2.8. Assessment of 3A cells viability

Trypan-blue exclusion method was used to assess viability of 3A cells at semi-confluence (70–80%) or 48 h after confluence, using the TC10 Automated Cell Counter (Biorad, Italy).

2.9. Statistical analysis

All data are expressed as mean ± SD. Student's *t*-test was used to compare means between groups, as indicated in the legend of the figures. *P* value was considered significant $\leqslant 0.05$. All statistical analyses were performed using GraphPad Prism software.

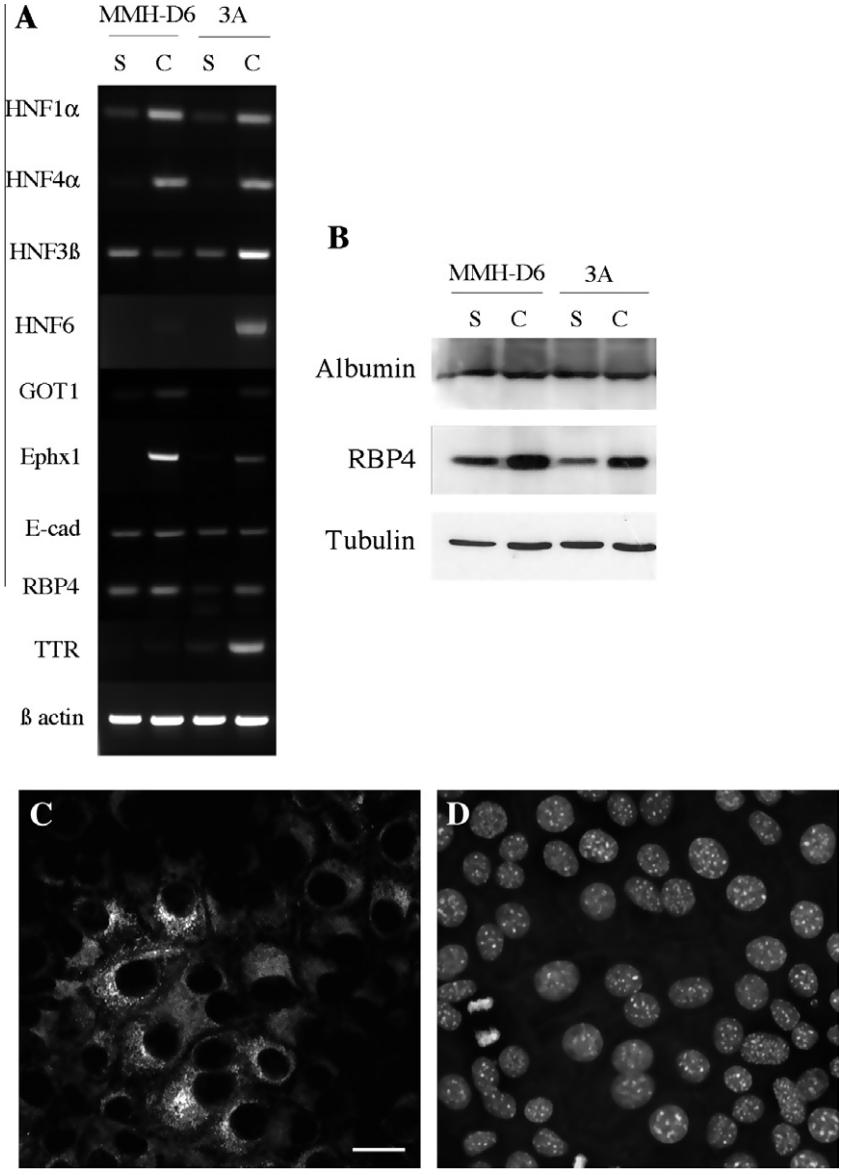

Fig. 1. Expression of hepato-specific genes in three murine liver cell lines. (A) The two hepatic clonal cell lines derived from transgenic (MMH-D6) or wild type (3A) mice were grown in two different conditions: sub-confluent (s) and confluent (c). RNA extracted from MMH-D6 and 3A cells was used in a PCR assay to evaluate the expression of the genes indicated. Data shown are representative of at least three independent experiments. (B) 40 μg of total cell lysates of the two cell clones were fractionated by 4–20% SDS–PAGE and analysed by Western blotting and chemiluminescence. Blot is representative of at least three independent experiments. Confocal microscopy of cells immunostained for albumin (C) and counterstained with DAPI to visualize the nuclei (D). Magnification bar = 20 μm.

3. Results

3.1. Characterization of 3A cells

3.1.1. Expression of liver-specific genes and proteins

3A cells, established from wild type mice liver, were tested and compared with a clonal cell lines derived from transgenic mice (MMH-D6) (Amicone et al., 1995) for their capacity to express liver specific genes; MMH-D6 cells have previously been characterized as an immortalized, untransformed and differentiated hepatocytic cell line (Mancone et al., 2010) and have thus been used as control cells in this study. Fig. 1A shows a panel containing the key hepato-specific genes analysed by PCR assay in MMH-D6 and 3A cells under different growth conditions: sub-confluent (s) and 48 h after confluence (c). When confluent, the two cell lines expressed hepatocyte nuclear factors (HNF1α, HNF4α, HNF3β, HNF6), glutamate oxaloacetate transaminase (GOT1), epoxide hydrolase (Ephx1), E-cadherin (E-cad), RBP4 and transthyretin (TTR); confluent MMH-D6 cells showed lower expression of HNF6 and TTR genes compared to 3A cells. The expression of these genes in both cell lines was low or undetectable in the sub-confluent state. The expression of two hepatic secretory proteins, albumin and RBP4, was analysed by Western blotting and is shown in Fig. 1B. Both albumin and RBP4, two of the most representative proteins in the adult liver, were synthesised by the two cell lines. RBP4 was more abundantly expressed in confluent cells in both lines. Albumin expression and intracellular localization were also examined by confocal laser scanning microscopy in 3A cells (Fig. 1C).

3.1.2. Morphological features

To study the morphology of 3A cells, fluorescence staining of F-actin and ß-catenin was performed and analysed by confocal laser scanning microscopy. As shown in Fig. 2, F-actin (A, C) and ß-catenin (B, D) were correctly organized. Both proteins showed a stronger signal close to the cell membrane outlining the cellular morphology. In the orthogonal projection F-actin appeared to be concentrated along the cell periphery but also showed some cytoplasmic staining, while β-catenin showed stronger staining in the apical part of the cells close to the plasma membrane. Confluent 3A cells exhibited a polygonal-hexagonal shape typical of epithelial cells. The z-stack analysis (Fig. 2C–F) shows the cuboidal structure of these cells and indicates that they formed a continuous and morphologically homogenous monolayer.

3.1.3. Fluorescein secretion assay

3A cells, as shown in Fig. 3, were able to internalize FDA that underwent intracellular hydrolysis and was secreted as fluorescein into intercellular spaces corresponding to bile canaliculi-like spaces (in Fig. 3A–D). This localization of fluorescein was also suggested by the orthogonal projection from the z-stack of 3A cell monolayer (Fig. 3E), where concentration of secreted fluorescein in specific areas between the cells was observed in cell monolayers counterstained with cell membrane staining using a fluorescent WGA conjugate, that selectively binds to *N*-acetylglucosamine and *N*-acetylneuraminic acid (sialic acid) residues.

3.1.4. Periodic Acid Schiff's (PAS) glycogen staining assay

Glycogen synthesis and accumulation was tested in 3A cells by PAS staining (Fig. 4) and viewed by transmitted light microscopy (A) and by fluorescence microscopy (C), taking advantage of the inherent fluorescence of the Schiff reagent in stained cells (Pilling et al., 2010). As shown by both methods, glycogen accumulation was observed in the majority of cells, although clusters of cells throughout the monolayer appeared more intensely stained. Specificity of staining was determined by digestion of glycogen with α-amylase (diastase) prior to PAS treatment, which eliminated the purple staining (B) or auto-fluorescence (D) specific for glycogen.

3.1.5. Retinol availability regulates RBP4 secretion

Modulation of RBP4 secretion by its ligand, retinol, is a documented feature of mature hepatocytes. 3A cells retained the regulated secretion of RBP4 as demonstrated by Western blot analysis

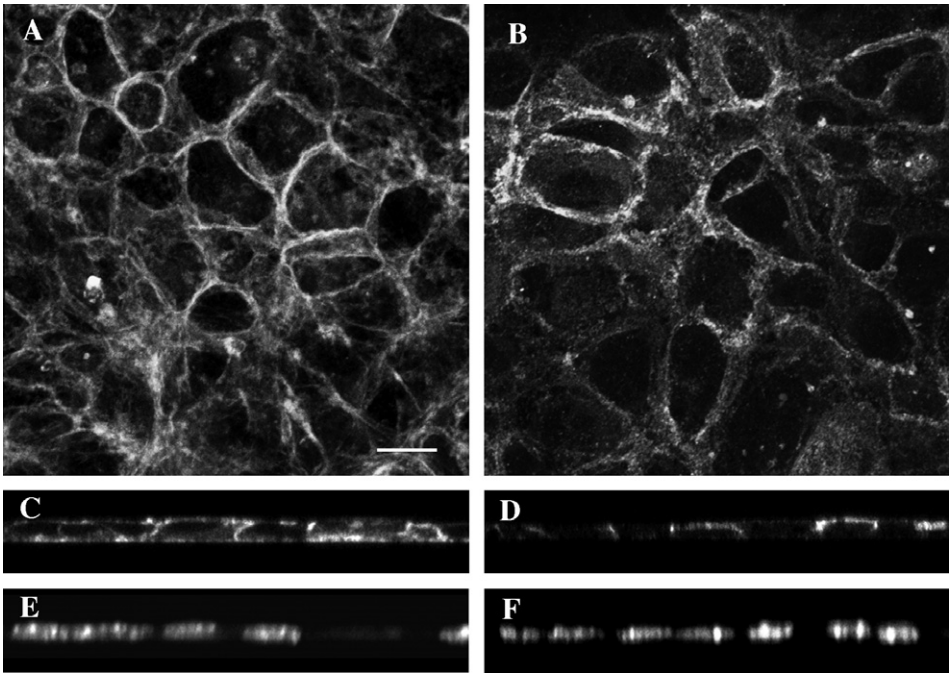

Fig. 2. Analysis of 3A cells morphology. Confocal microscopy of confluent 3A cells stained for F-actin (A, C, E) and β-catenin (B, D, F). Maximal intensity projection (MIP) of 25 0.25 μm thick *Z*-plane image sections (A, B) and representative orthogonal projections from the z-stack are shown for F-actin (C) and β-catenin (D) with their corresponding nuclear staining (E, F) Magnification bar = 20 μM.

of cell lysates and immunoprecipitation in culture media (Fig. 5). Retinol deprivation caused inhibition of RBP4 secretion, therefore the amount of RBP4 detected in lysates of 3A cells grown for 48 h in delipidized medium (−) was significantly higher than in control 3A cells, grown in the same delipidized medium in which 3 μM retinol was added (+). Tubulin was immunostained in the same cell lysates as loading control. As expected, the amount of RBP4 detected by immunoprecipitation in the culture media was higher in cells grown in the presence of retinol, in which RBP4 secretion is efficient, compared to cells grown in retinol deficiency, in which RBP4 secretion is impaired.

3.2. Response to tunicamycin treatment

To evaluate the stress response to an inducer of protein misfolding, 3A cells were incubated with 5 μg/ml TM for 4 h and total RNA was extracted and analysed with a UPR Pathway Real Time-PCR Array (SA Biosciences Qiagen Italia, Italy). As shown in Fig. 6A, TM treatment modulated the expression of different genes involved in cellular functions linked to the stress response. In the graph are indicated the genes with a fold change >2 compared to control cells not treated with TM. Fig. 6B shows that TM treatment caused a shift in electrophoretic mobility of both IRE1α and PERK compared to control cells, indicative of the phosphorylation of these two proteins (Harding et al., 1999), and stimulated the expression of CHOP that in control conditions – i.e. not stressed – was undetectable. In addition, upon TM treatment and IRE1 activation, digestion of the PCR amplified XBP1 cDNA by the restriction enzyme PstI was inhibited, as shown in Fig. 6C.

4. Discussion

3A cells were isolated from 14.5 dpc embryo of a wild type mouse strain and spontaneously immortalized. Their viability, tested by trypan-blue exclusion, was >90% after 48 h at confluence (data not shown), and these were the conditions used in all further experiments. The morphological features of 3A cells were highlighted by staining the cytoskeletal protein F-actin and the junctional protein ß-catenin. ß-catenin is part of the adherens junctions and is involved in the stabilization of the epithelial monolayer, in anchoring to the F-actin cytoskeleton and in transmitting the signals that cause cells to stop dividing once the cells reach confluence (Perez-Moreno et al., 2008). Recent evidence suggests that β-catenin plays also an important role in various aspects of liver biology, including development (both embryonic and postnatal), regeneration, HGF-induced hepatomegaly, zonation and cancer pathogenesis (Thompson and Monga, 2007). Our analysis by confocal laser microscopy indicates that the overall shape and structural organization of 3A cells is similar to that of primary hepatocytes (Schmelz et al., 2001). Moreover, these cells grow on

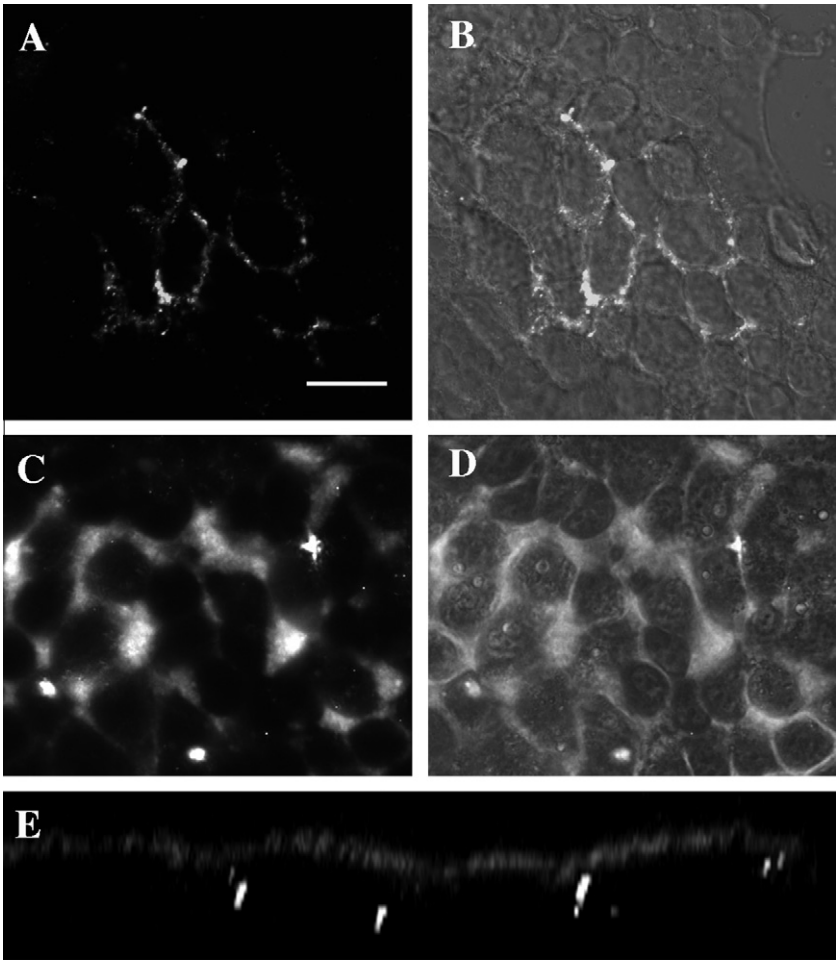

Fig. 3. 3A cells excrete fluorescein in bile canaliculi-like structures. Cells were treated with FDA and analysed after 30 min at 37 °C by confocal microscopy (A, B) or by fluorescence (C, D) microscopy. Merge with differential interference contrast (DIC) confocal image (C) or phase-contrast image (D) or are also shown. A representative orthogonal projection from a confocal z-stack of cells treated with FDA (white aggregates between cells) and counter-stained with WGA for cell membranes (gray apical staining) is shown in (E). Magnification bar = 20 μM.

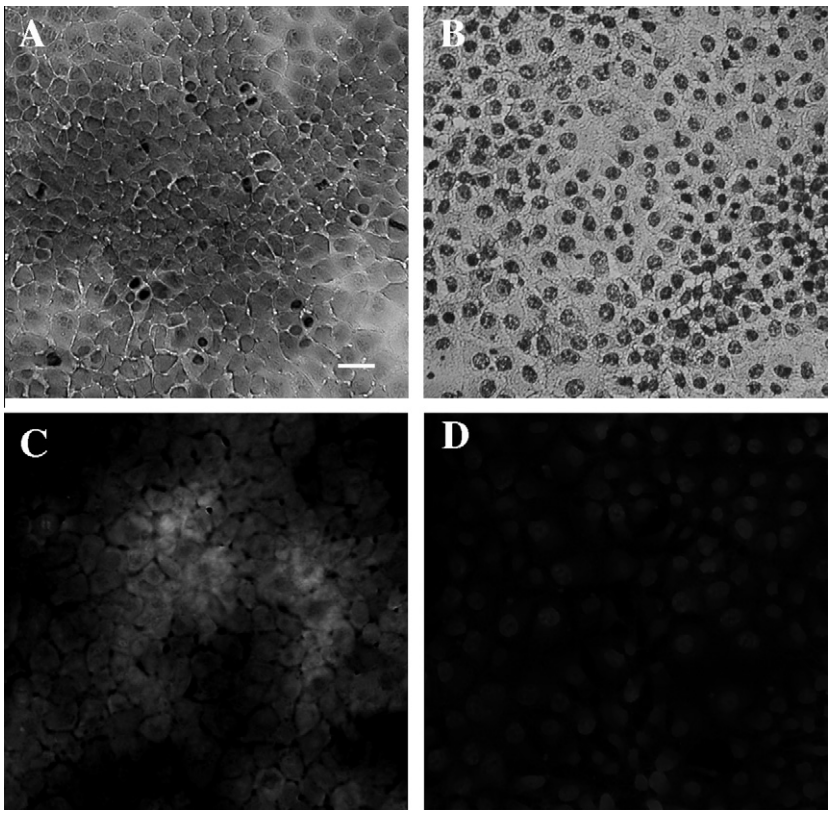

Fig. 4. Confluent 3A cells synthesize and accumulate glycogen. Glycogen storage in 3A cells was detected both by PAS (A), that gives an intense intracellular staining, and by auto-fluorescence emitted by the Schiff reagent used in PAS staining procedure (C). As a control of specificity, cells were treated with diastase to digest glycogen before PAS staining (B, D). Magnification bar = 20 μM.

collagen substrate mainly as a monolayer, as determined by z-stack analysis of confocal images. PCR analysis was carried out in sub-confluent and confluent growth conditions, to confirm previous findings in MMH cells in which terminal differentiation program is stimulated by cell–cell contact (Mancone et al., 2010). PCR results demonstrated that 3A cells express several liver key genes and, in particular, specific transcription factors (Hepatocyte Nuclear Factors, HNF) such as HNF1, that regulates hepatocyte polarization and contributes to the transcriptional regulation of genes crucial for carbohydrate synthesis and storage, lipid metabolism, detoxification and serum protein synthesis (Guguen-Guillouzo and Guillouzo, 2010), and HNF4α, a key regulator of morphological and functional hepatocytes differentiation and polarization (Parviz et al., 2003). Furthermore, 3A cells express enzymes involved in amino acid and xenobiotic metabolism (GOT1, Ephx1), proteins implicated in cell–cell contacts (E-cadherin) and proteins that transport micronutrients such as vitamin A or thyroid hormone (RBP4 and TTR, respectively). The expression of RBP4 was also demonstrated by protein immunoblotting and was higher in confluent than in sub-confluent cells. As demonstrated by immunofluorescence and Western blotting experiments, 3A cells expressed albumin, considered a late hepatic marker (Conigliaro et al., 2008; De Kock et al., 2009).

FDA staining is a useful tool to verify the functionality of hepatocytes and to detect the formation of bile canaliculi-like structures. Hepatocytes excrete endogenous and exogenous compounds into bile canaliculi by two main transporters, the multidrug resistance protein-2 (Mrp2) and the bile-salt export pump (Bsep), both localized at the "canalicular domains" of cell membrane, that function as efflux pumps and actively extrude substrates into the bile (Sidler Pfandler et al., 2004). FDA is not fluorescent and is able to permeate cell membranes by simple

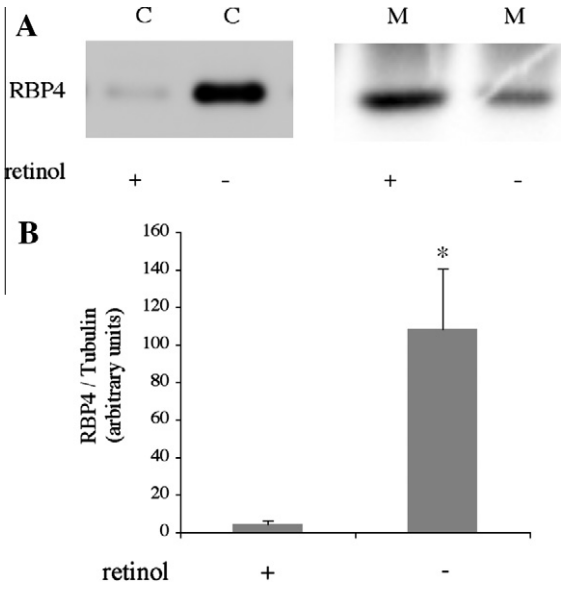

Fig. 5. Retinol deficiency inhibits in 3A cells RBP4 secretion. (A) Cells were incubated for 48 h in delipidized serum in the presence (+) or in the absence (−) of 3 μM retinol, culture media were harvested and subjected to immunoprecipitation with anti-RBP4 antibody, while cells were lysed in RIPA buffer. 40 μg of total cell lysates (C) and immunoprecipitated media (M) were fractionated by 4–20% SDS–PAGE and RBP4 was detected by Western blotting with specific primary antibody followed by chemiluminescence. (B) RBP4 intracellular amount respect to tubulin (not shown) was measured by ImageQuantTL software. A representative blot is shown and the densitometric analysis represents three independent experiments performed in triplicate. Data are expressed as means ± SD and p value $\leqslant 0.05$ is considered significant (Student's t-test).

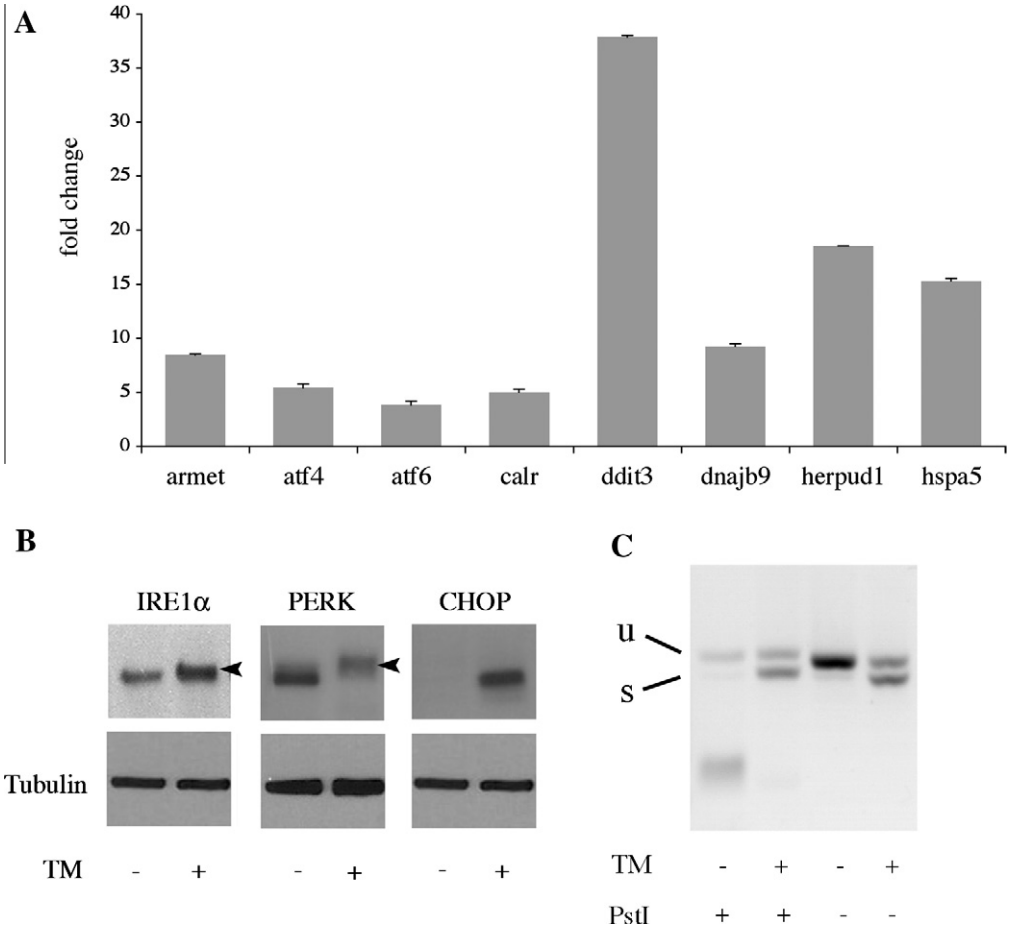

Fig. 6. Tunicamycin treatment induces an UPR response in 3A cells. (A) Specific UPR genes activation by TM treatment was analysed performing a UPR Pathway RT-PCR Array in samples treated or not (control) with TM. Genes that changed >2-folds between treated and control cells were considered and represented in the graph. Real Time-qPCR results were calculated using the $2^{-\Delta\Delta Ct}$ method. The genes presented were significantly modulated with a p value $\leqslant 0.05$ (Student's t-test). (B) Cells were treated with TM for 4 h (+) or not treated (−), then 40 μg of total cell lysates in each lane were fractionated by SDS–PAGE and the proteins indicated in the figure were visualized with specific primary antibodies by Western blotting and chemiluminescence; tubulin was included as a protein loading control. Arrowheads indicate the phosphorylated forms of IRE1α and PERK, characterized by a slightly slower migration rate. Blot is representative of at least three independent experiments. (C) Total RNA was extracted from cells previously subjected (+) or not (−) to TM treatment and XBP-1 gene was amplified by PCR; XBP-1 PCR fragment was then subjected to digestion with the restriction enzyme PstI and analysed on 1% agarose gel (panel C). Unspliced (u) and spliced (s) forms are indicated.

diffusion; it undergoes intracellular hydrolysis to fluorescent fluorescein and is then addressed for excretion into bile canaliculi (Gebhardt and Jung, 1982). The data obtained in this study by FDA staining demonstrated that confluent 3A cells are able to secrete molecules into extracellular spaces that are equivalent to bile canaliculi, suggesting a correct functional organization. This secretory activity is, in fact, preserved *in vitro* only in mature hepatocytes and in highly differentiated hepatic cell lines (Shanks et al., 1994), even though the complex network of bile canaliculi observed in the liver can be reproduced only in tridimensional hepatocyte culture models, such as proliferating small hepatocytes colonies (Sidler Pfandler et al., 2004) or primary hepatocytes grown in a collagen sandwich (Liu et al., 1999), in which the tissue organization is maintained.

Glycogen synthesis and accumulation is a typical function of some cell types, including hepatocytes, as an efficient storage system for excessive glucose. 3A cells were shown to accumulate glycogen, another marker of hepatic function. Moreover, we have demonstrated that 3A cells exhibit regulated accumulation and secretion of RBP4 depending on ligand availability, a typical feature of mature hepatocytes. Regulated RBP4 secretion from hepatocytes by retinol was initially described in animals (Perozzi et al., 1991), while it is not maintained in some tumoural hepatic cell lines such as HepG2 (Bellovino et al., 1999). 3A cells are therefore an appropriate model to shed light on mechanisms that control RBP4 secretion and metabolic pathways modulated during vitamin A deficiency.

To further investigate the potential of the 3A hepatic cell model, we have studied their response to stress stimuli, in particular TM treatment, looking at the modulation of several genes specifically involved in the so-called Unfolded Protein Response, UPR. High throughput technologies, as PCR Arrays, offer the possibility of a wide scale analysis of genes involved in specific pathways in a single sample. By simultaneously screening the genes represented in the UPR Pathway Real Time-PCR Array, we observed the activation of a specific response to TM in 3A cells. This response included the modulation of genes involved in protein folding, ubiquitination, Endoplasmic Reticulum-Associated protein Degradation (ERAD) and apoptosis. Among them, we detected the strong activation of *ddit3* gene, that encodes for CCAAT/-enhancer-binding protein homologous protein (CHOP). GRP78 (*hspa5*) and Herp (*herpud1*) were also strongly up-regulated, as expected since these two proteins are master regulators of protein folding and of ERAD, respectively (Ma and Hendershot, 2004; Hendershot, 2004). The ER is an essential cellular compartment for protein synthesis, maturation and secretion, as well as for Ca^{2+} storage. Upon accumulation of

unfolded/misfolded proteins or induction of stress by various conditions, such as inflammation, excess of nutrients, etc., a cascade of events leads to the regulation of specific genes involved in the restoration of ER homeostasis. The UPR pathway is initiated by the combined action of some key proteins that act both as sensors of ER stress and response transducers. GRP78, that exerts essential functions in protein folding as molecular ER chaperone, is probably the main "sensor" of ER stress; ATF6, IRE-1 and PERK are the "transducers", responsible for the communication between stressed ER and the cytosol/nucleus, through a series of other molecules. Their concerted activity leads to a reduction of protein load in the ER through the attenuation of protein synthesis, followed by an increase in the folding/degradation capacity of the cell through the up-regulation of specific ER chaperones; finally, if homeostasis cannot be restored, cells are addressed to programmed death by apoptosis. Overall, these mechanisms are integrated to provide a response that remodels the secretory apparatus and cellular physiology, according to the demands imposed by ER stress (Kaufman et al., 2002).

TM is a drug that blocks protein glycosylation, generating massive glycoproteins misfolding and ER stress, that in turn activates UPR. We have used TM treatment to check the capacity of 3A cells to cope with ER overload and protein misfolding. IRE1, PERK and CHOP, the three key proteins that trigger this kind of response, were activated upon TM treatment. Activation is carried out by two different mechanisms: IRE1 and PERK, despite the total protein amount is not modulated by the treatment, are activated by phosphorylation; CHOP expression, that in control conditions is undetectable, is strongly stimulated. We found that in 3A cells treated with TM, IRE1 and PERK underwent phosphorylation (Harding et al., 1999), as suggested by the shift in molecular weight due to the increase of molecular weight; CHOP protein expression was strongly stimulated, confirming at the protein level the induction observed at the RNA level (Fig. 6B). IRE1 phosphorylation, promoted by stress, in turn stimulated the activation of XBP1, a transcription factor involved in the UPR (Yoshida, 2007). In a specific region of this gene, removed upon mRNA splicing by IRE1, there is a cutting site for the PstI restriction enzyme, therefore resistance of XBP1 to PstI digestion suggests a response to stress, as we have found in 3A cells treated with TM (Fig. 6C). Recent evidences suggest that the unspliced form of XBP1 is a feedback negative regulator of the spliced form in the cytoplasm, such that the expression of the two forms of XBP1 is switched in response to the ER condition (Yoshida et al., 2006). Preservation of this mechanism in 3A cells further strengthens their suitability for studies of hepatic stress response. This type of response has been studied in different hepatic models. In particular, primary hepatocytes (Pfaffenbach et al., 2010) and cell lines such as HepG2 were shown to be acceptable *in vitro* models for UPR (Di Fazio et al., 2010). However, HepG2 are of tumoral origin and do not preserve many regulated functions, as demonstrated for modulation of RBP4 secretion by retinol availability (Bellovino et al., 1999) or for mechanism of ceruloplasmin secretion (Pisu et al., 2005).

The importance of having a hepatic cell line that responds properly to UPR is related to the essential role that this mechanism exerts during cell life. Several evidence suggest that UPR is involved not only in the response to an acute exogenous stress, but is also necessary to maintain homeostasis of cellular functions during normal physiological fluctuations, in particular in highly secretory cells as B lymphocytes (Iwakoshi et al., 2003) and pancreatic ß-cells (Back et al., 2009).

UPR also plays a critical role in the progression of a wide variety of diseases. Several authors have demonstrated that in liver, as well as in other tissues, it has a fundamental role in influencing metabolic functions, such as lipogenesis and glucose homeostasis (Rutkowski et al., 2008), and in the induction of pathological states such as Non-Alcoholic Fatty Liver Disease and altered glucose tolerance (Szczesna-Skorupa et al., 2004; Oyadomari et al., 2008; Kammoun et al., 2009; Zheng et al., 2010) and some cancers (Lee, 2007). Interestingly, different animal and cellular models have been used to test the activity of specific molecules, the so-called *chemical chaperones*, able to reduce ER stress and therefore to restore cellular homeostasis (Ozcan et al., 2006).

In conclusion, 3A cells can be considered a useful hepatocyte model that preserves several important liver characteristics, particularly suitable for studies related to ER stress response and for testing molecules with potential *chemical chaperone* activity.

5. Conflict of interest statement

None declared.

Acknowledgements

We thank Prof. Sancia Gaetani for her invaluable support and suggestions. We acknowledge financial support by grant "NUME" (DM3888/7303/08) from the Italian Ministry of Agriculture, Food & Forestry (MiPAAF).

References

Amicone, L., Galimi, M.A., Spagnoli, F.M., Tommasini, C., De Luca, V., Tripodi, M., 1995. Temporal and tissue-specific expression of the MET ORF driven by the complete transcriptional unit of human A1AT gene in transgenic mice. Gene 162 (2), 323–328.

Back, S.H., Scheuner, D., Han, J., Song, B., Ribick, M., Wang, J., Gildersleeve, R.D., Pennathur, S., Kaufman, R.J., 2009. Translation attenuation through eIF2alpha phosphorylation prevents oxidative stress and maintains the differentiated state in beta cells. Cell Metab. 10 (1), 13–26.

Bellovino, D., Lanyau, Y., Garaguso, I., Amicone, L., Cavallari, C., Tripodi, M., Gaetani, S., 1999. MMH cells: an in vitro model for the study of retinol-binding protein secretion regulated by retinol. J. Cell. Physiol. 181 (1), 24–32.

Conigliaro, A., Colletti, M., Cicchini, C., Guerra, M.T., Manfredini, R., Zini, R., Bordoni, V., Siepi, F., Leopizzi, M., Tripodi, M., Amicone, L., 2008. Isolation and characterization of a murine resident liver stem cell. Cell Death Differ. 15 (1), 123–133.

De Kock, J., Vanhaecke, T., Biernaskie, J., Rogiers, V., Snykers, S., 2009. Characterization and hepatic differentiation of skin-derived precursors from adult foreskin by sequential exposure to hepatogenic cytokines and growth factors reflecting liver development. Toxicol. In Vitro 23 (8), 1522–1527.

Di Fazio, P., Schneider-Stock, R., Neureiter, D., Okamoto, K., Wissniowski, T., Gahr, S., Quint, K., Meissnitzer, M., Alinger, B., Montalbano, R., Sass, G., Hohenstein, B., Hahn, E.G., Ocker, M., 2010. The pan-deacetylase inhibitor panobinostat inhibits growth of hepatocellular carcinoma models by alternative pathways of apoptosis. Cell. Oncol. 32 (4), 285–300.

Ferrini, J.B., Pichard, L., Domergue, J., Maurel, P., 1997. Long-term primary cultures of adult human hepatocytes. Chem. Biol. Interact. 107 (1–2), 31–45.

Gebhardt, R., Hengstler, J.G., Muller, D., Glockner, R., Buenning, P., Laube, B., Schmelzer, E., Ullrich, M., Utesch, D., Hewitt, N., Ringel, M., Hilz, B.R., Bader, A., Langsch, A., Koose, T., Burger, H.J., Maas, J., Oesch, F., 2003. New hepatocyte in vitro systems for drug metabolism: metabolic capacity and recommendations for application in basic research and drug development, standard operation procedures. Drug Metab. Rev. 35 (2–3), 145–213.

Gebhardt, R., Jung, W., 1982. Biliary secretion of sodium fluorescein in primary monolayer cultures of adult rat hepatocytes and its stimulation by nicotinamide. J. Cell Sci. 56, 233–244.

Guguen-Guillouzo, C., Guillouzo, A., 2010. General review on in vitro hepatocyte models and their applications. Methods Mol. Biol. 640, 1–40.

Harding, H.P., Zhang, Y., Ron, D., 1999. Protein translation and folding are coupled by an endoplasmic-reticulum-resident kinase. Nature 397 (6716), 271–274.

Hendershot, L.M., 2004. The ER function BiP is a master regulator of ER function. Mt. Sinai J. Med. 71 (5), 289–297.

Hewitt, N.J., Lechon, M.J., Houston, J.B., Hallifax, D., Brown, H.S., Maurel, P., Kenna, J.G., Gustavsson, L., Lohmann, C., Skonberg, C., Guillouzo, A., Tuschl, G., Li, A.P., LeCluyse, E., Groothuis, G.M., Hengstler, J.G., 2007. Primary hepatocytes: current understanding of the regulation of metabolic enzymes and transporter proteins, and pharmaceutical practice for the use of hepatocytes in metabolism, enzyme induction, transporter, clearance, and hepatotoxicity studies. Drug Metab. Rev. 39 (1), 159–234.

Iwakoshi, N.N., Lee, A.H., Vallabhajosyula, P., Otipoby, K.L., Rajewsky, K., Glimcher, L.H., 2003. Plasma cell differentiation and the unfolded protein response intersect at the transcription factor XBP-1. Nat. Immunol. 4 (4), 321–329.

Kammoun, H.L., Chabanon, H., Hainault, I., Luquet, S., Magnan, C., Koike, T., Ferre, P., Foufelle, F., 2009. GRP78 expression inhibits insulin and ER stress-induced

SREBP-1c activation and reduces hepatic steatosis in mice. J. Clin. Invest. 119 (5), 1201–1215.
Kaufman, R.J., Scheuner, D., Schroder, M., Shen, X., Lee, K., Liu, C.Y., Arnold, S.M., 2002. The unfolded protein response in nutrient sensing and differentiation. Nat. Rev. Mol. Cell Biol. 3 (6), 411–421.
Lee, A.S., 2007. GRP78 induction in cancer: therapeutic and prognostic implications. Cancer Res. 67 (8), 3496–3499.
Liu, X., LeCluyse, E.L., Brouwer, K.R., Gan, L.S., Lemasters, J.J., Stieger, B., Meier, P.J., Brouwer, K.L., 1999. Biliary excretion in primary rat hepatocytes cultured in a collagen-sandwich configuration. Am. J. Physiol. 277 (1 Pt 1), G12–G21.
Ma, Y., Hendershot, L.M., 2004. Herp is dually regulated by both the endoplasmic reticulum stress-specific branch of the unfolded protein response and a branch that is shared with other cellular stress pathways. J. Biol. Chem. 279 (14), 13792–13799.
Mancone, C., Conti, B., Amicone, L., Bordoni, V., Cicchini, C., Calvo, L., Basulto Perdomo, A., Fimia, G.M., Tripodi, M., Alonzi, T., 2010. Proteomic analysis reveals a major role for contact inhibition in the terminal differentiation of hepatocytes. J. Hepatol. 52, 234–243.
Oyadomari, S., Harding, H.P., Zhang, Y., Oyadomari, M., Ron, D., 2008. Dephosphorylation of translation initiation factor 2alpha enhances glucose tolerance and attenuates hepatosteatosis in mice. Cell Metab. 7 (6), 520–532.
Ozcan, U., Yilmaz, E., Ozcan, L., Furuhashi, M., Vaillancourt, E., Smith, R.O., Gorgun, C.Z., Hotamisligil, G.S., 2006. Chemical chaperones reduce ER stress and restore glucose homeostasis in a mouse model of type 2 diabetes. Science 313 (5790), 1137–1140.
Parviz, F., Matullo, C., Garrison, W.D., Savatski, L., Adamson, J.W., Ning, G., Kaestner, K.H., Rossi, J.M., Zaret, K.S., Duncan, S.A., 2003. Hepatocyte nuclear factor 4alpha controls the development of a hepatic epithelium and liver morphogenesis. Nat. Genet. 34 (3), 292–296.
Perez-Moreno, M., Song, W., Pasolli, H.A., Williams, S.E., Fuchs, E., 2008. Loss of p120 catenin and links to mitotic alterations, inflammation, and skin cancer. Proc. Natl. Acad. Sci. USA 105 (40), 15399–15404.
Perozzi, G., Mengheri, E., Colantuoni, V., Gaetani, S., 1991. Vitamin A intake and in vivo expression of the genes involved in retinol transport. Eur. J. Biochem. 196 (1), 211–217.
Pfaffenbach, K.T., Gentile, C.L., Nivala, A.M., Wang, D., Wei, Y., Pagliassotti, M.J., 2010. Linking endoplasmic reticulum stress to cell death in hepatocytes: roles of C/EBP homologous protein and chemical chaperones in palmitate-mediated cell death. Am. J. Physiol. Endocrinol. Metab. 298 (5), E1027–E1035.
Pilling, J., Garside, H., Ainscow, E., 2010. Development of a quantitative 96-well method to image glycogen storage in primary rat hepatocytes. Mol. Cell. Biochem. 341 (1–2), 73–78.
Pisu, P., Bellovino, D., Gaetani, S., 2005. Copper regulated synthesis, secretion and degradation of ceruloplasmin in a mouse immortalized hepatocytic cell line. Cell Mol. Biol. (Noisy-le-grand) (Suppl. 51), OL859–OL867.
Ron, D., Walter, P., 2007. Signal integration in the endoplasmic reticulum unfolded protein response. Nat. Rev. Mol. Cell Biol. 8 (7), 519–529.
Rutkowski, D.T., Wu, J., Back, S.H., Callaghan, M.U., Ferris, S.P., Iqbal, J., Clark, R., Miao, H., Hassler, J.R., Fornek, J., Katze, M.G., Hussain, M.M., Song, B., Swathirajan, J., Wang, J., Yau, G.D., Kaufman, R.J., 2008. UPR pathways combine to prevent hepatic steatosis caused by ER stress-mediated suppression of transcriptional master regulators. Dev. Cell 15 (6), 829–840.
Schmelz, M., Schmid, V.J., Parrish, A.R., 2001. Selective disruption of cadherin/catenin complexes by oxidative stress in precision-cut mouse liver slices. Toxicol. Sci. 61 (2), 389–394.
Schroder, M., Kaufman, R.J., 2005. The mammalian unfolded protein response. Annu. Rev. Biochem. 74, 739–789.
Shanks, M.R., Cassio, D., Lecoq, O., Hubbard, A.L., 1994. An improved polarized rat hepatoma hybrid cell line. Generation and comparison with its hepatoma relatives and hepatocytes in vivo. J. Cell Sci. 107 (Pt 4), 813–825.
Sidler Pfandler, M.A., Hochli, M., Inderbitzin, D., Meier, P.J., Stieger, B., 2004. Small hepatocytes in culture develop polarized transporter expression and differentiation. J. Cell Sci. 117 (Pt 18), 4077–4087.
Szczesna-Skorupa, E., Chen, C.D., Liu, H., Kemper, B., 2004. Gene expression changes associated with the endoplasmic reticulum stress response induced by microsomal cytochrome p450 overproduction. J. Biol. Chem. 279 (14), 13953–13961.
Thompson, M.D., Monga, S.P., 2007. WNT/beta-catenin signaling in liver health and disease. Hepatology 45 (5), 1298–1305.
Yoshida, H., 2007. ER stress and diseases. FEBS J. 274 (3), 630–658.
Yoshida, H., Oku, M., Suzuki, M., Mori, K., 2006. PXBP1(U) encoded in XBP1 pre-mRNA negatively regulates unfolded protein response activator pXBP1(S) in mammalian ER stress response. J. Cell Biol. 172 (4), 565–575.
Zheng, Z., Zhang, C., Zhang, K., 2010. Role of unfolded protein response in lipogenesis. World J. Hepatol. 2 (6), 203–207.